NJC

Accepted Manuscript

This is an *Accepted Manuscript*, which has been through the Royal Society of Chemistry peer review process and has been accepted for publication.

Accepted Manuscripts are published online shortly after acceptance, before technical editing, formatting and proof reading. Using this free service, authors can make their results available to the community, in citable form, before we publish the edited article. We will replace this *Accepted Manuscript* with the edited and formatted *Advance Article* as soon as it is available.

You can find more information about *Accepted Manuscripts* in the Information for Authors.

Please note that technical editing may introduce minor changes to the text and/or graphics, which may alter content. The journal's standard Terms & Conditions and the Ethical guidelines still apply. In no event shall the Royal Society of Chemistry be held responsible for any errors or omissions in this *Accepted Manuscript* or any consequences arising from the use of any information it contains.

ROYAL SOCIETY OF CHEMISTRY

www.rsc.org/njc

Table of contents

for

Gold nanoparticles-based enhanced ELISA for respiratory syncytial virus

Lei Zhan, [a] Wen Bi Wu, [b] Xiao Xi Yang, [b] and Cheng Zhi Huang*[a b]

[a]*Key Laboratory on Luminescent and Real-Time Analytical Chemistry (Southwest University), Ministry of Education, College of Chemistry and Chemical Engineering, Southwest University, Chongqing 400715, China*

[b]*College of Pharmaceutical Sciences, Southwest University, Chongqing 400715, China*

Fax: +86-23-68866796; Tel: +86-23-68254659; E-mail: chengzhi@swu.edu.cn

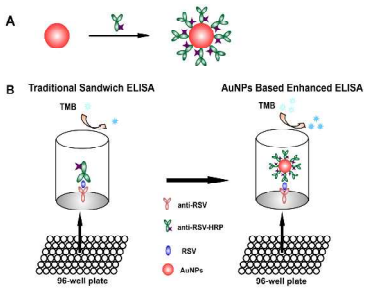

A highly sensitive colorimetric immunoassay for the detection of RSV by adopting AuNPs as a multienzyme carrier was developed.

Cite this: DOI: 10.1039/c0xx00000x

www.rsc.org/xxxxxx

ARTICLE TYPE

Gold nanoparticles-based enhanced ELISA for respiratory syncytial virus

Lei Zhan,[a] Wen Bi Wu,[a,b] Xiao Xi Yang,[b] and Cheng Zhi Huang*[a,b]

Received (in XXX, XXX) Xth XXXXXXXXX 20XX, Accepted Xth XXXXXXXXX 20XX

DOI: 10.1039/b000000x

Respiratory syncytial virus (RSV) mediates severe respiratory illness in infants and young children worldwide, and it is also a significant pathogen of the elderly and immune compromised. Due to low infectious dose and high infectious rate of RSV, remarkably rapid and sensitive RSV detection is important to infection control and antiviral drugs discovery. In this work, we described a highly sensitive enzyme-linked immunosorbent assay (ELISA) utilizing gold nanoparticles (AuNPs) for the detection of RSV. Gold nanoparticles were used as carriers of the signalling antibody anti-RSV-HRP (horseradish peroxidase) in order to achieve an amplification of the signal. Compared to conventional ELISA procedures, this assay resulted in higher sensitivity and shorter assay time in the range between 0.5 and 50 pg/mL. The application of AuNPs to the enhanced ELISA showed acceptable reproducibility, stability, and could be readily applied to other pathogens determination in clinical diagnostics.

Introduction

Respiratory syncytial virus (RSV), a negative sense single-stranded RNA virus in the *Paramyxoviridae* family, has been long recognised as the primary cause of serious viral lower respiratory tract illness in infants and young children worldwide.[1] According to the Centers for Disease Control and Prevention (CDC), RSV remains the most important cause of bronchiolitis and pneumonia in children under 1 year of age, responsible for emergency room visits and hospitalization.[2] In the USA alone, it is estimated that between 85 000 to 144 000 infants are admitted to the hospital with respiratory symptoms.[3] In addition, RSV can cause serious complications in the elderly people[4] and those adults with cardiopulmonary diseases[5] or immunocompromised.[6] Globally, disease burden associated RSV infection is estimated at 64 million cases and 160 000 deaths every year.[7] Since RSV is extremely contagious and since no safe and effective vaccine is available at present, the development of simple, fast and sensitive methods would be of paramount importance for the early detection of RSV infection, essential for the timely and effective diagnosis and therapy monitoring.

So far, the laboratory diagnosis of RSV infection has been generally made by virus isolation, detection of the viral antigen or viral specific RNA in respiratory secretions.[8] Among them, isolation of RSV in tissue culture have been considered as "gold standard" for confirmation of RSV infection in a long period of time,[9] because it is effective and often complementary. However, this procedure is time-consuming (3-6 days), laborious and may require experienced staff to perform. The need for rapid, sensitive, specific procedures for the detection of RSV has led to the development of methods which do not rely on cell culture techniques, such as reverse transcription and polymerase chain reaction (RT-PCR) for the detection of viral specific nucleic acid sequences.[10] Unfortunately, most PCR methods require some costly equipment and are not suitable for use outside the laboratory.

Enzyme-linked immunosorbent assay (ELISA) is the technique most commonly used as a diagnostic tool or a quality control check for antigens detection and quantification owing to its simplicity, low cost, readability and acceptability.[11] ELISA tests are based on the antibody-antigen specific binding, involving four steps: (1) immobilizing capture antibody on a solid surface support (such as a microtiter plate); (2) incubating with antigen-containing sample; (3) binding the antigen with an enzyme labeled antibody; and (4) adding a chromogenic substrate for this enzyme to generate a measurable signal. Of the three commonly used enzyme labels in ELISA (horseradish peroxidase (HRP), alkaline phosphatase (ALP), and β-galactosidase), HRP is the most desirable antibody label because it is the smallest and most stable of the three.[12] It catalyzes the oxidation of many reducing substrates such as 3, 3', 5, 5'-tetramethybenzidine (TMB), 2,2-azino-bis(3-ethylbenzthiazoline-6-sulfonic acid) (ABTS), and *O*-phenylenediamine (OPD) by H_2O_2. These methods offer simplicity in operation and can be performed outside of the laboratory to provide a rapid diagnosis, but the sensitivity represents a considerable shortcoming.

To improve the detection sensitivity of ELISA, incorporation of an additional signal amplification step is necessary. Many efforts have been made to improve the sensitivity by using various signal amplification strategies such as tyramide signal amplification technique,[13] liposomes[14] and nanomaterials (metal nanoparticles, carbon-based nanostructures and magnetic nanoparticles)[15] amplification system. In particular, gold nanoparticles (AuNPs) are very attractive materials because of

their facile synthesis, large surface area-to-volume ratio, high loading capacity, chemical stability and biocompatibility.[16] Hence, AuNPs-based immunoassays have been extensively explored and applied in clinical diagnostics, food safety and environmental monitoring. In these assays, the AuNPs are employed as the signal indicators[17] or served as carriers to load more signalling molecules, leading to high sensitivity.[18] On the basis of these work, we designed a highly sensitive immunoassay for RSV detection by combining the unique property of AuNPs with the well-established optical ELISA test. The use of AuNPs as a multi anti-RSV-HRP carrier offered an enhanced performance for RSV determination in comparison with the traditional ELISA, and could be easily extended to other pathogens detection.

Experimental

Materials

All chemicals were of analytical grade and were used as received without further purification. Polyclonal (goat) anti-RSV (ab20745) and Polyclonal (goat) anti-RSV-HRP conjugated (ab20686) were purchased from abcam plc (U.K.). Bovine serum albumin (BSA) and trisodium citrate were obtained from Beijing Dingguo Changsheng Biotechnology Co. Ltd (Beijing, China). Hydrogen peroxide was purchased from Chuandong Chemical (Group) Co., Ltd. (Chongqing, China). 3,3',5,5'-tetramethylbenzidine (TMB) was obtained from Aladdin Chemistry Co., Ltd (Shanghai, China), Chloroauric acid tetrahyrate ($HAuCl_4\ 4H_2O$) was purchased from Sinopharm Chemical Reagent Co. Ltd (Shanghai, China). Ultrapure water used for whole experiment was purified by a Milli-Q filtration system (Millipore, USA). 96-well ELISA microtiter plates (Corning-Costar, 25922) were purchased from Corning Inc. (New York, USA).

The coating buffer consisted of 0.05 M carbonate/bicarbonate buffer (pH 9.6). The phosphate buffer solution (PBS) consisted of 0.15 M NaCl, 2 mM KCl and 0.02 M phosphate buffer (pH 7.4). Blocking buffer solution consisted of a PBS solution with 5% (w/v) BSA (pH 7.4). The washing buffer consisted of a PBS solution with 0.05% Tween 20. All aqueous solutions were prepared using ultrapure water (Mill-Q, Millipore, 18.2 M)

Instruments

JEM-2010 transmission electron microscopy (TEM) was used to identify the size and shape of AuNPs. The absorption spectra of AuNPs were measured with U-3010 UV-vis spectrophotometer (Hitachi, Japan). The optical density (OD) at 450 nm was recorded by a Biotek Microplate Reader (USA).

Preparation of RSV

HEp-2 cells were cultured in RPMI 1640 medium supplemented with 2% fetal bovine serum and then incubated at 37 ℃ with 5% CO_2. RSV stock was prepared by infecting a confluent T-25 flask of HEp-2 cells with RSV. Infection was performed with thawed virus in cell medium. Following the initial infection, cells were incubated for 2h, after which 5 mL of cell medium was added to the flask. The infection was allowed to proceed for 6 days, after which cells were scraped from the surface of the flask. The supernatant containing the cells was collected and centrifuged for 10 min at 3000 rpm. Following removal of the supernatant, the cell pellet was resuspended in 2 mL PBS buffer. The cells were then frozen at -80 ℃. Then the cells were thawed at room temperature. The freezing/thawing cycle was repeated two times to ensure the release of virus particles from the cell wall. After the second cycle, the cells were centrifuged at 3000 rpm for 10 min to remove large cellular debris. The supernatant was then separated into aliquots of 1 mL and stored at -80 ℃. The concentration of RSV was assessed by commercial kit.

Synthesis and characterization of gold nanoparticles

Gold nanoparticles were prepared according to the classical citrate reduction (Frens method) with slight modifications.[19] In brief, first, all glassware and magnetic stirring bars used in experiments were cleaned with aqua regia (3:1 v/v HCl (37%)/HNO_3 (65%)) solutions, rinsed thoroughly with distilled water, and then oven-dried prior to use. Second, 4 mL of 1% (w/v) $HAuCl_4\ 4H_2O$ in 98 mL of ultrapure water was boiled at continuous stirring in a 250 mL round-bottom flask equipped with a condenser to maintain a constant volume. Then, 11.4 mL of 1% (w/v) trisodium citrate solution was quickly added to the boiling solution, and kept boiling for another 20 min. The solution colour changed from gray to blue, then purple, and finally to wine red during this period. After cooling down, the as-prepared citrate-AuNPs solution was filtered through a 0.22 μm nylon membrane to remove any large aggregates. Using Beer's law, the concentration of the as-prepared AuNPs solution was determined to be 4.7 nM (ε=2.7×10^8 M^{-1} cm^{-1}). Then, an aqueous solution of AuNPs (1 nM) was adjusted to pH 9.0 with NaOH and stored at 4 ℃ for further use.

Preparation of the Au-anti-RSV-HRP conjugate

The optimum conditions including the pH value and antibody concentration for the preparation of the Au-anti-RSV-HRP complex was determined by a salt induced aggregation test. A schematic of the complex preparation is given in Figure 1A. Precisely, 9 μL of anti-RSV-HRP solution at a concentration of 20 μg/mL was added to 211 μL of the AuNPs solution. The mixture was incubated at room temperature for 30 min, and then added into 220 μL buffer. After 30 min, the solution was centrifuged at 15000 g for 15 min to remove the excess of antibody. The precipitated gold conjugates were resuspended in 220 μL buffer solution.

Sandwich enzyme-based immunoassay

For RSV detection, 96-well microtiter plate was first modified with anti-RSV antibody (100 μL) in coating buffer at 4 °C overnight. After washing the plates three times with washing buffer, the plates were blocked with blocking buffer for 1 h at 37 °C. Subsequently, the plates were washed three times with washing buffer, and then the capture antibody coated and blocked plates were stored at 4 °C and sealed with parafilm until use. 100 μL virus diluted in buffer (pH 7.4) to the desired concentrations (0, 0.5, 1, 5, 10, 25, 50 pg/mL) was added to wells and kept at 37 °C for 1h. The wells were then rinsed three times with washing buffer and 100 μL anti-RSV-HRP or Au-anti-RSV-HRP was added to each well, incubated at 37 °C for 1h, rinsed with washing buffer and patted dry. 100 μL substrate solutions consisted of 0.3 mM TMB and 64 μM H_2O_2 was added to each well and reacted for 30 min at 37 °C. The reaction was stopped by adding 50 μL 1 mol/L H_2SO_4 and recorded at 450 nm.

Results and discussion

Principle of AuNPs-based enhanced ELISA

The principle of AuNPs-based enhanced optical immunoassay is based on adopting AuNPs as carriers of signalling antibody anti-RSV-HRP (horseradish peroxidase) in the classical sandwich ELISA procedure. Conventional ELISA tests are always carried out by using HRP-labeled antibody, which can catalyze the oxidation of TMB by H_2O_2 to generate coloured products. Quantitative analysis of the coloured products may be recorded on a microplate reader, thus providing a convenient approach for detecting RSV. Because of their tremendous surface area, AuNPs could bind with more HRP-labeled antibody molecules, which can generate a significant amplification for the catalytic reaction when compared to conventional ELISA. As illustrated in Scheme 1A, Au-anti-RSV-HRP complexes were prepared through simple physical adsorption. And the 96-well microplate was first immobilized with the capture antibody. Then, the target virus captured on the substrate was then detected by its immunoreactions with Au-anti-RSV-HRP complexes (Scheme 1B). Due to the design of the AuNPs carrier, RSV could be detected with high sensitivity.

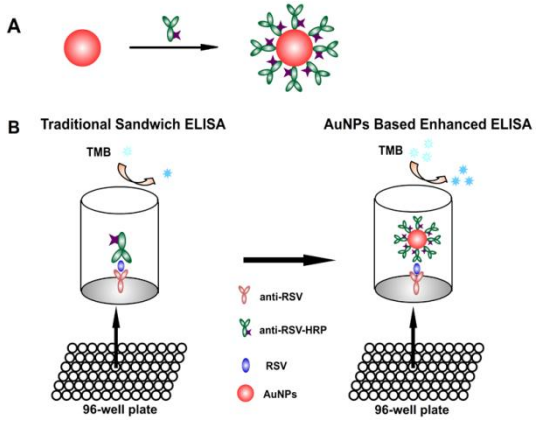

Scheme. 1 Schematic of the preparation of Au-anti-RSV-HRP complex (A) and the sandwich-type ELISA procedure for RSV detection using AuNPs-based probe compared with traditional ELISA (B).

Characterization of the Au-anti-RSV-HRP conjugates

UV-vis spectroscopy was employed to analyze the bare AuNPs and obtained Au-anti-RSV-HRP conjugates. As shown in Fig. 1A, bare AuNPs displayed a characteristic plasmon absorption peak at 518 nm, while a red shift to 522 nm was attributed to the immobilization of HRP-labelled anti-RSV antibody onto the AuNPs.[20] To confirm the quality of AuNPs after antibody coating, the AuNPs were characterized by TEM imaging. Fig. 1B showed the colloid AuNPs before coupling with anti-RSV-HRP antibody. The average size of these particles was about 13 nm and they tended to suffer from a slight agglomeration in the buffer solution. When functionalized with antibody, though the average diameter had no obvious change, they were well-dispersive (Fig. 1C), indicating that adsorption of anti-RSV-HRP could facilitate the dispersion and stability of AuNPs.[21] Dynamic light scattering (DLS) was further performed to determine the hydrodynamic diameter of AuNPs before and after coupling with anti-RSV-HRP (Fig. S1, ESI†). The average hydrodynamic diameter of AuNPs was 22.4 ± 0.27 nm. However, the average hydrodynamic diameter increased to 27.2 ± 0.32 nm after the anti-RSV-HRP functionalization, demonstrating that the anti-RSV-HRP was indeed adsorbed onto AuNPs surfaces. Zeta potential measurement described the surface charge variations of AuNPs. Initially, the surface potential of bare AuNPs was -49.5 ± 0.87 mV because the citrate capped the surface of the nanoparticles. When antibody was adsorbed onto the surfaces, the charge of the nanoparticles was almost unchanged (-45.2 ± 2.17 mV), most likely owing to the acidic groups in antibody. Taking the above data together, they indicated that anti-RSV-HRP was successfully immobilized on AuNPs surfaces.

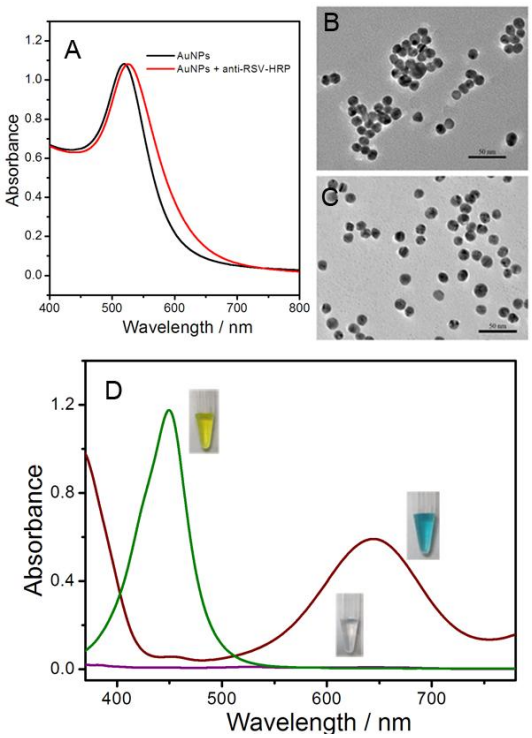

Fig. 1 Characterization of AuNPs and Au-anti-RSV-HRP conjugate. A. UV-vis spectra of AuNPs and Au-anti-RSV-HRP conjugate. B, C. TEM images of AuNPs and Au-anti-RSV-HRP conjugates. D. Colour reaction of TMB catalyzed by the Au-anti-RSV-HRP conjugates in the presence H_2O_2 (the purple line is absorption spectrum of the reaction solution without the presence of Au-anti-RSV-HRP complexes; the red and green line are absorption spectra of the reaction solution mixed with AuNPs-anti-RSV-HRP before and after addition of H_2SO_4, respectively.

After obtaining the Au-anti-RSV-HRP conjugates, we demonstrated that adsorbed HRP enzymes maintained their activities by using the colour reaction of TMB in the presence of H_2O_2. As seen in Fig. 1D, the mixture solution of TMB and H_2O_2 turned from clear to blue and had a major absorbance peak at 652 nm when Au-anti-RSV-HRP conjugates were introduced. The colour development was stopped by the addition of acid, changing the colour to yellow (with a maximum absorbance at 450 nm). The colour change induced by this reaction indicated that Au-anti-RSV-HRP conjugates had catalytic activities and could be used in ELISA by replacing anti-RSV-HRP. Besides, it has been reported that citrate-capped AuNPs possessed catalytic activity as the peroxidase mimics.[22] To evaluate the synergistic effect of AuNPs and HRP, we compared the catalytic activity of bare AuNPs, pure HRP and Au-anti-RSV-HRP conjugates (Fig. S2, ESI†). The result showed that Au-anti-RSV-HRP conjugates

haven't enhanced colorimetric responses, suggesting that bare AuNPs exhibited limited catalytic activity under applied reaction conditions and acted as carriers only in the ELISA test.

Optimization of the assay condition

The assay sensitivity is affected by several factors such as the concentration of anti-RSV-HRP, the pH for conjugation and the concentration of Au-anti-RSV-HRP complex.

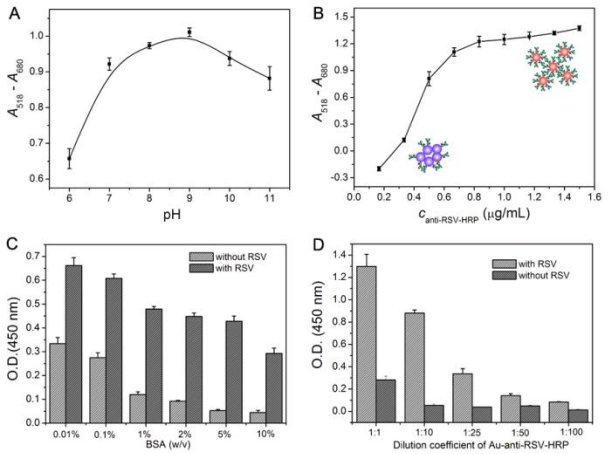

Fig. 2 Optimization of the assay conditions. (A) pH optimization for the preparation of the Au-anti-RSV-HRP conjugates; (B) Gold aggregation test performed to judge the minimum antibody concentration for conjugation; (C) Optimization of BSA concentration for blocking the nonspecific binding sites; (D) Optimization of the concentration of the Au-anti-RSV-HRP conjugates to be used in the ELISA test.

It is well known that the stability of 13 nm AuNPs is associated with the concentrations of electrolytes in solution, even very low concentrations of salt could induce irreversible aggregation of such AuNPs, accompanying by a colour change from red to blue.[23] However, they became more stable and can withstand high NaCl concentration when biomolecules (DNA, protein) were first adsorbed.[24] Therefore, the salt-induced gold aggregation test was performed to verify the optimal pH for the conjugation of anti-RSV-HRP detecting antibody to AuNPs (Fig. 2A). Precisely, after synthesis, the AuNPs solution pH was adjusted to 6, 7, 8, 9, 10 and 11 before incubation with the antibody. The optimal pH at which the antibody more efficiently prevented gold aggregation resulted to be around 9, ensuring the highest level of gold surface coverage by the antibody.

The antibody concentration which prevented gold aggregation was also determined by measuring the difference between the absorbance at 518 and 680 nm and plotting it against the concentration used (Fig. 2B). Under the optimal pH for conjugation, the minimum antibody concentration to use for conjugation was 0.82 μg/mL, corresponding to the number of anti-RSV-HRP molecules of 4 for each AuNPs. Meanwhile, it can be seen that the spectra of AuNP-anti-RSV-HRP conjugate solutions became more and more similar to that of bare AuNPs with the increase of anti-RSV-HRP (Fig. S3, ESI†), indicating that the surface was fully covered.

BSA is a classic blocking agent and has been used extensively as a blocker in immunoassay. In this system, the effect of BSA concentration on sensitivity of the assay was tested by varying the BSA concentration in the blocking buffer. As shown in Fig. 2C, the background decreased slowly with increasing BSA concentration and then reached a plateau. Though the signal of RSV-mediating decreased gradually, the best performance was achieved when blocking the Au-anti-RSV-HRP conjugate with 5% BSA.

The concentration of the AuNP-anti-RSV-HRP conjugates to be used in the ELISA test was also optimized (Fig. 2D). It was found using the 1:1 diluted Au conjugates resulted in a high nonspecific signal, which recorded by the high value of OD even when no RSV was added. When dilutions of the Au conjugates were taken, the nonspecific signal was reduced. However, when a 1: 100 diluted Au conjugates was used, very low signal was noted. The best dilution, with a good balance between low nonspecific signal and high sensitivity, was 1: 10.

Comparison with classical ELISA test

Later, we compared the detection performance of the conventional anti-RSV-HRP probe with our Au-anti-RSV-HRP probe. Fig. 4 summarized the performance of the two probes in the ELISA test.

As depicted clearly by the OD values, the AuNPs-based probe showed much higher ELISA signals than that of the conventional probe. The limit of detection (LOD) of the AuNPs-based probe was found to be about 0.5 pg/mL, which is exceeds the LOD of the conventional ELISA probe (25 pg/mL) by 50 times, proving the superiority of the current approach. The improvement of the LOD for the AuNPs-based ELISA strategy is the consequence of introducing AuNPs as carriers for amplification. It was also noteworthy that AuNPs-based assay was able to quantify RSV very rapidly within 5 min, whereas the traditional ELISA usually required 15-30 min for colour signal development. The sensitivity of the newly developed ELISA is extremely attractive because the concentration of RSV in the early stage of infection is too low to be monitored.

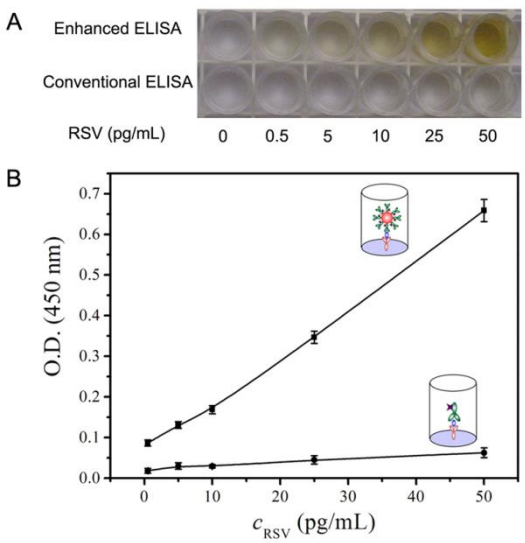

Fig. 3 ELISA test performed for RSV detection. (A) Image of the ELISA results from 0 pg/mL to 50 pg/mL of RSV per well. (B) Comparison of the detection performance in the presence and absence of AuNPs by plotting absorbance intensity at 450 nm *versus* various concentration of RSV in PBST solutions.

Specificity, reproducibility and stability

To demonstrate the specificity of the proposed ELISA for RSV detection, the Au-anti-RSV-HRP complex was employed to

detect other samples including H9N2 influenza virus, inactivated RSV (RSV-M), human epithelial type 2 (Hep2) cells, gram-negative bacteria *Escherichia Coli* (*E. Coli*), fetal bovine serum (FBS), and RPMI-1640 medium following the same procedure as above. Since the microplate was initially coated with the RSV-specific antibody, the unmatched virus, bacteria, cells, FBS and medium did not cause the colour change eventually by showing a similar level of OD value to the negative control. It has to be pointed out that there was no false positive found using the inactivated RSV, which was destroyed and couldn't replicate. In the case of RSV, however, OD value enhancement in excess of 10-fold was observed compared with other samples, suggesting that the AuNPs-based enhanced immunoassay could perform a good specificity for RSV detection.

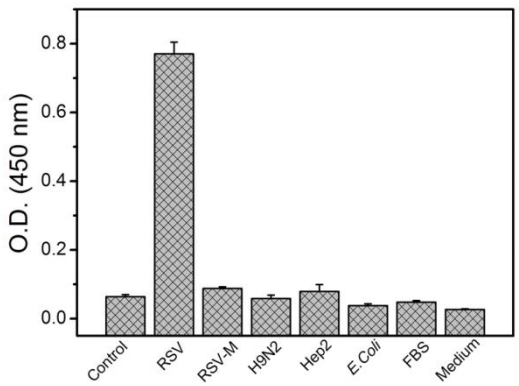

Fig. 4 Selectivity of the proposed enhanced immunoassay for RSV. The concentration of RSV-M was 90 pg/mL; H9N2 virus was kindly donated by Wuhan Institute of Virology, Chinese Academy of Sciences; the number of Hep2 cells and *E. Coli* was 10^5/mL and 10^6/mL, respectively.

The reproducibility of the assay was investigated with intra-assay and inter-assay precision. Taking 10 pg/mL of RSV for example, the intra-assay of the AuNPs-based ELISA was evaluated for five replicate measurements one time and the inter-assay was estimated with five times made at the same system. The intra- and inter-assay variation coefficients obtained were 2.97 % and 4.39 %, indicating good reproducibility of the protocol described above.

The stability of the synthesized Au-anti-RSV-HRP complex was also investigated by ELISA detection 10 pg/mL of RSV through sandwich immunoreactions (Fig. S4, ESI†). When the complex was stored at 4 ℃, no obvious decrease in intensity was observed after 3 weeks of storage, which indicated that the prepared immunoprobe possessed good storage stability and potential for practical application.

Conclusions

In this work, we successfully developed an enhanced ELISA for RSV by incorporating AuNPs as carriers of the signalling antibody. The detection limit of this approach was found to be 50-fold lower than those of the conventional HRP-based immunoassay. The high sensitivity of this probe is based on the high loading amount of proteins onto AuNPs surfaces. Such improved detection systems would enable diagnosis and detection of RSV infection at their early stages in clinical applications, thus providing improved therapeutic outcomes. Additionally, the detection was performed in microplate, which is the most popular detection format in clinical laboratories, making this assay low-cost and easily adaptable into currently available diagnostic platforms.

Acknowledgements

This work was supported by National Basic Research Program of China (973 Program, 2011CB933600).

Notes and references

[a] *Key Laboratory on Luminescence and Real-Time Analytical Chemistry (Southwest University), Ministry of Education, College of Chemistry and Chemical Engineering, Southwest University, Chongqing 400715, China. E-mail: chengzhi@swu.edu.cn; Fax: +86 23 68367257; Tel: +86 23 68254659*

[b] *College of Pharmaceutical Science, Southwest University, Chongqing 400716, China.*

† Electronic Supplementary Information (ESI) available: [details of any supplementary information available should be included here]. See DOI: 10.1039/b000000x/

1 R. A. Tripp, *Viral Immunol*, 2004, **17**, 165-181; R. Rudraraju, B. G. Jones, R. Sealy, and J. L. Hurwitz, *Viruses*, 2013, **5**, 577-594.

2 CDC, 2009, http://www.cdc.gov/rsv/index.html.

3 D. K. Shay, R. C. Holman, R. D. Newman, L. L. Liu, J. W. Stout and L. J. Anderson, *JAMA*, 1999, **282**, 1440-1446.

4 D. G. Garvie and J. Gray, *Br Med J*, 1980, **281**,1253-1254; A. R. Falsey and E. E. Walsh, *Drugs & Aging*, 2005, **22**, 577-587.

5 E. E. Walsh, A. R. Falsey and P. A. Hennessey, *Am J Resp Crit Care*, 1999, **160**, 791-795.

6 J. A. Englund, C. J. Sullivan, M. C. Jordan, L. P. Dehner, G. M. Vercellotti and H. H. Balfour Jr, *Ann Intern Med*, 1988, **109**, 203-208; J. O Ebbert and A. H. Limper, *Respiration*, 2006, **72**, 263-269.

7 WHO, 2009, http://apps.who.int/vaccine_research/diseases/ari/en/index2.html.

8 T. Popow-Kraupp and J. H. Aberle, *Open Microbiol J*, 2011, **5**, 128-134; C. Prendergast and J. Papenburg, *Future Microbiol*, 2013, **8**, 435-444.

9 R. C. Welliver, *Clin Microbiol*, 1988, **1**, 27-39; A. P. Borek, S. H. Clemens, V. K. Gaskins, D. Z. Aird and A. Valsamakis, *J Med Virol*, 2006, **44**, 1105-1107.

10 J. H. Henkel, S. W. Aberle, M. Kundi and T. Popow-Kraupp, *J Med Virol*, 1997, **53**, 366-371; E. E. Walsh, A. R. Falsey, I. A. Swinburne and M. A. Formica, *J Med Virol*, 2001, **63**, 259-263; P. Jokela, H. Piiparinen, K. Luiro and M. Lappalainen, *Clin Microbiol Infec*, 2010, **16**, 1568-1573.

11 T. Porstmann and S. T. Kiesig, *J Immunol Methods*, 1992, **150**, 5-21; C. P. Jia, X. Q. Zhong, B. Hua, M. Y. Liu, F. X. Jing, X. H. Lou, S. H. Yao, J. Q. Xiang, Q. H. Jin and J. L. Zhao, *Biosens Bioelectron*, 2009, **24**, 2836-2841.

12 S. S. Deshpande, *Enzyme Immunoassays: From Concept to Product Development*, Kluwer Academic Publisher, Dordrecht, 1996.

13 D. Saha, D. Acharya, D. Roy and T. K. Dhar, *Anal. Bioanal. Chem.*, 2007, **387**, 1121-1130; A. E. Niotis, C. Mastichiadis, P. S. Petrou, I. Christofidis, S. E. Kakabakos, A. Siafaka-Kapadai and K. Misiakos, *Anal. Bioanal. Chem.*, 2010, **396**, 1187-1196; L. Yuan, L. Xu and S. Liu, *Anal. Chem.*, 2012, **84**, 10737-10744.

14 K. A. Edwards and J. C. March, *Anal. Biochem.*, 2007, **368**, 39-48; R. Genc, D. Murphy, A. Fragoso, M. Ortiz and C. K. O'Sullivan, *Anal Chem*, 2011, **83**, 563-570; U. Ruktanonchai, O. Nuchuchua, R. Charlernroj, T. Pattarakankul and N. Karoonuthaisiri, *Anal Biochem*, 2012, **429**, 142-147.

15 A. Ambrosi, M. T. Castañeda, A. J. Killard, M. R. Smyth, S. Alegret and A. Merkoçi, *Anal. Chem.*, 2007, **79**, 5232-5240; A. Ambrosi, F. Airò and A. Merkoçi, *Anal. Chem.*, 2010, **82**, 1151-1158; F. Zhou, M. Wang, L. Yuan, Z. Cheng, Z. Wu and H. Chen, *Analyst*, 2012, **137**, 1779-1784; Q. Zhang, B. Zhao, J. Yan, S. Song, R. Min and C. Fan, *Anal. Chem.*, 2011, **83**, 9191-9196; H. Lin, Y. Liu, J. Huo, A. Zhang,

Y. Pan, H. Bai, Z. Jiao, T. Fang, X. Wang, Y. Cai, Q. Wang, Y. Zhang and X. Qian, *Anal. Chem.*, 2013, **85**, 6228-6232.
16 R. A. Sperling, P. R. Gil, F. Zhang, M. Zanella and W. J. Parak, *Chem. Soc. Rev.*, 2008, **37**, 1896-1908; E. Boisselier and D. Astruc, *Chem. Soc. Rev.*, 2009, **38**, 1759-1782; K. Saha, S. S. Agasti, C. Kim, X. Li and V. M. Rotello, *Chem. Rev.*, 2012, **112**, 2739-2779.
17 Y. Niu, Y. Zhao and A. Fan, *Anal. Chem.*, 2011, **83**, 7500-7506; C. Wang, D. Liu and Z. Wang, *Chem. Commun.*, 2012, **48**, 8392-8394.
18 K. C. Han, E. G. Yang and D. R. Ahn, *Chem. Commun.*, 2012, **48**, 5895-5897; Z. Gao, M. Xu, Li. Hou, G. Chen and D. Tang, *Anal. Chem.*, 2013, **85**, 6945-6952; D. Liu, X. Huang, Z. Wang, A. Jin, X. Sun, L. Zhu, F. Wang, Y. Ma, G. Niu, A. R. H. Walker and X. Chen, *ACS Nano*, 2013, **7**, 5568-5576.
19 G. Frens, *Nat Phys Sci*, 1973, **241**, 20-22; Y. Wang, Y. F. Li, J. Wang, Y. Sang and C. Z. Huang, *Chem. Commun.*, 2010, **46**, 1332-1334.
20 S. Kumar, J. Aaron and K. Sokolov, *Nat Protoc*, 2008, **3**, 314-320; C. Thiruppathiraja, V. Saroja, S. Kamatchiammal, P. Adaikkappan and M. Alagar, *J. Environ. Monit.*, 2011, **13**, 2782-2787.
21 V. D. Pham, H. Hoang, T. H. Phan, U. Conrad and H. H. Chu, *Adv. Nat. Sci.: Nanosci. Nanotechnol*, 2012, **3**, 045017. B. Masereel, M. Dinguizli, C. Bouzin, N. Moniotte, O. Feron, B. Gallez, T. V. Borght, C. Michiels and S. Lucas, *J. Nanopart. Res*, 2011, **13**, 1573-1580; M. Arruebo, M. Valladares and Á. González-Fernández, *J. Nanomater.*, 2009, **2009**, 1-24.
22 Y. J. Long, Y. F. Li, Y. Liu, J. J. Zheng, J. Tang and C. Z. Huang, *Chem. Commun.*, 2011, **47**, 11939-11941.
23 M. Liu, C. Jia, Q. Jin, X. Lou, S. Yao, J. Xiang and J. Zhao, *Talanta*, 2010, **81**, 1625-1629; X. Zhang, M. R. Servos and J. Liu, *J. Am. Chem. Soc.*, 2012, **134**, 7266-7269.
24 H. D. Hill and C. A. Mirkin, *Nat Protoc*, 2006, **1**, 324-336; Y. Sang, L. Zhang, Y. F. Li, L. Q. Chen, J. L. Xu and C. Z. Huang, *Anal Chim Acta*, 2010, **659(1-2)**, 224-228.

